JOURNAL OF GUIDANCE, CONTROL, AND DYNAMICS
Vol. 33, No. 3, May–June 2010

# Simulations of Quasi-Satellite Orbits Around Phobos

Paulo J. S. Gil*
*Instituto Superior Técnico, 1049-001 Lisbon, Portugal*
and
Julia Schwartz†
*ESA, 64293 Darmstadt, Germany*

DOI: 10.2514/1.44434

**In this work, quasi-synchronous orbits around Phobos are studied from a preliminary mission design point of view. Addressed issues include stability of the orbits, possible choices of specific suitable orbits, and their impact on the design of a mission to Phobos (eclipses, observation conditions, etc.). An exploration of the phase space is performed to assess the precision requirements on the initial conditions of the spacecraft state vector for insertion into these orbits. The possibility of using an orbit outside the orbital plane of Phobos around Mars is also explored.**

## Nomenclature

| | | |
|---|---|---|
| $e$ | = | second primary (usually Phobos) orbit eccentricity in the three-body problem |
| $h_{\max}$, $h_{\min}$ | = | maximum and minimum altitudes, relative to Phobos, reached by a quasi-satellite orbit, km |
| $R_{\mathrm{Ph}}$ | = | mean radius of Phobos, km |
| $T_{\mathrm{Ph}}$ | = | mean sidereal period of revolution of Phobos |
| $v_x$, $v_y$, $v_z$ | = | spacecraft velocity Cartesian components in the synodic reference frame, m/s |
| $x$, $y$, $z$ | = | spacecraft position vector Cartesian components in the synodic reference frame, km |
| $\alpha$, $\beta$, $\gamma$, $\delta$, $\psi$ | = | parameters defining the quasi-satellite orbit geometry |
| $\mu$ | = | second primary mass, divided by the total mass, in the three-body problem |

## I. Introduction

THE Martian moon Phobos is possibly a captured asteroid, making it an interesting destination for scientific missions. Understanding its basic scientific nature could provide insights into the evolution of the planets and small bodies of our solar system [1].

At the same time, it is much easier to approach and return from Phobos than from most asteroids because of Mars's low orbital inclination with respect to the ecliptic and its distance to the sun [2].

To land on Phobos, however, it is crucial to first determine an adequate landing site, which requires orbiting the moon and performing observations from a distance. It also requires the development of an approach and, in the case of a sample return mission (SRM), an escape strategy, and the assessment of important mission events such as eclipses and Earth occultations.

Orbiting Phobos in a Keplerian-type way is not possible because the mass of Phobos is too small, in relation with its close distance to Mars, to outweigh the disturbing gravitational attraction of Mars. This is illustrated by the fact that, in the context of the three-body problem, the Lagrange points are very close to the surface of Phobos and the region of influence of Phobos ends below its surface.

It is nevertheless possible to orbit Phobos in a special kind of orbit [3], designated as a distant retrograde orbit (DRO), which is a particular family of the distant satellite orbits [4] (DSOs), also referred to as quasi-synchronous orbits or quasi-satellite orbits [5] (QSO). QSOs exist beyond the Lagrange points, as seen from the rotating synodic reference frame usually used in three-body problems. In this frame, a coplanar QSO relative to the orbital plane of Phobos can be described as an elliptical reference trajectory drifting mainly back and forth in the direction of the orbital velocity of Phobos. In the inertial reference, the spacecraft (S/C) is still orbiting Mars with its orbit slightly perturbed by Phobos. In some cases, this motion can resemble the epicycloidal motion in the old Ptolemaic system, with the important difference that in this case it is a dynamic effect originated by the existence of Phobos. Because each ellipsoidal drifting trajectory (as seen in the synodic reference frame) is not an orbit in the usual sense of a possibly perturbed Keplerian trajectory, some authors called it *epicycle* [4], and we will adopt this term for the rest of this work for convenience of description. Hence, we will refer to the ellipselike orbit of the S/C around Phobos in the synodic reference frame as an epicycle, whereas a QSO refers to the entire dynamics of the drifting epicycles.

This paper examines the problem of finding sufficiently stable QSOs around Phobos and selecting them to meet the defined objectives. It also discusses mission-analysis-related aspects of the orbits, such as eclipse and occultation durations, surface illumination, and ground track. Considering that the polar regions of Phobos may be of special scientific interest to the mission, orbits going outside Phobos's orbital plane to high latitudes are investigated as well.

## II. Background

### A. Missions to Phobos

Two significant projects with Phobos as a destination exist: the former U.S.S.R. Phobos mission and the forthcoming Russian SRM Phobos–Grunt. Both include a mission stage during which probes orbit Phobos in a QSO.

#### 1. *Phobos 1 and 2*

The Phobos mission [2] was launched in 1988 and included two S/C: Phobos 1 and Phobos 2. The intention of the mission was to put two landers on the moon's surface, one to remain motionless and the other capable of hopping around on the surface to study the composition of the soil in various locations.

After Mars orbit insertion and corrections of the pericenter to come closer to the Phobos orbit, the S/C maneuvered to a circular orbit, similar but more inclined than that of Phobos. They were then supposed to be inserted into a QSO to circumnavigate Phobos. The distance to Phobos was between 200 and 600 km at this time. The QSO would have been almost coplanar with the moon's orbit around Mars. The next stage would have involved a transfer of the S/C to an

Presented as Paper 6429 at the AIAA/AAS Astrodynamics Specialist Conference and Exhibit 2008, Honolulu, HI, 18–21 August 2008; received 18 March 2009; revision received 18 January 2010; accepted for publication 19 January 2010. 

*Assistant Professor, Department of Mechanical Engineering, Avenue Rovisco Pais; Instituto de Engenharia Mecânica. Member AIAA.

†Flight Dynamics Engineer, European Space Operations Centre, Robert Bosch Strasse 5.

orbit even closer to Phobos and, afterward, a controlled approach to the moon to a height of 30–50 m. There, experiments were supposed to be performed and the landers deployed.

Unfortunately, both S/C were lost. Phobos 1 did not established radio contact due to a software upload that switched off the thrusters less than two months after launch. Phobos 2 reached the QSO insertion phase of the mission but also suffered a failure of the orientation control system due to an onboard computer malfunction. Despite the loss of the mission, it was reported [6] that the attained QSO was stable enough and that the S/C would have continued to circumnavigate Phobos for years.

#### 2. *Phobos–Grunt Sample Return Mission*

The Phobos–Grunt project is a Russian SRM [7] currently scheduled to be launched in 2011 by Russia.

Considerable work has been done in preparation of the Phobos–Grunt mission [8–11]. The scenario of this SRM, as described in [7], includes insertion into a QSO with epicycle dimensions of 50 km × 130 km [8] before landing on Phobos near the equatorial plane (0–30°) of latitude.

### B. Mission Design of a Sample Return Mission to Phobos

The general profile of an SRM to Phobos can be as follows:

1) Launch to a low Earth orbit, followed by insertion into an interplanetary trajectory to Mars.

2) Deceleration and Mars orbit insertion, typically into a highly eccentric elliptical orbit with the line of apsides in the orbital plane of Phobos to minimize fuel expenditure when maneuvering to approach the moon.

3) Inclination change to match the inclination of the orbit of Phobos, followed by reconnaissance at a certain distance to improve the ephemeris of Phobos and the relative position accuracy.

4) Insertion into a suitable proximity QSO to circumnavigate Phobos; observations with scientific objectives in mind, for example, cartography, as well as to check the selected landing site; landing preparation.

5) Landing on Phobos, operations on the surface, and launch from Phobos with the samples.

6) Escape from Phobos and insertion on a return interplanetary trajectory to Earth.

7) Reentry of the capsule containing the Phobos soil samples in the Earth atmosphere and recovery procedure.

This paper is concerned mainly with item 4, in particular, the selection of a suitable QSO satisfying operational requirements for the distance to Phobos, the period of revolution around Phobos, and, most importantly, the sufficient stability of the QSO. Special requirements for the landing procedure can also influence the choice of the QSO to be used. Eclipse and radio visibility requirements must be determined and taken into account as well, just like the visibility of the possible landing sites. This kind of study can support mission design choices and explore diverse possibilities such as using a QSO that goes outside the orbital plane of Phobos.

A QSO that remains approximately in the orbital $x$–$y$ plane of Phobos will be labeled a 2-D QSO. One with a three-dimensional geometry, in which the epicycles are inclined and extend considerably to the $z$ coordinate, will be designated as a 3-D QSO.

### C. Challenges in Orbiting Phobos

One difficulty that will most likely be encountered when trying to orbit Phobos in practice is the inaccurate knowledge of the relative position of the S/C with respect to the moon. Observations and orbit determination of the S/C and a check of the Phobos ephemeris must take place before a final approach commences. To ensure sufficient distance between the S/C and Phobos, the Phobos–Grunt project therefore foresees going into an orbit with a semimajor axis exceeding the semimajor axis of the Phobos orbit by as much as 500 km [8] before inserting the S/C into a QSO closer to Phobos.

**Table 1 Mars and Phobos selected data. The orbit of Phobos around Mars is almost equatorial and its period is about one-third of a day. Phobos is often described as an ellipsoid but the mean radius and the $J_2$ values are also indicated for reference**

| | Mars | Phobos |
|---|---|---|
| *Orbital parameters* | | |
| Semimajor axis, km | $2.2795 \times 10^8$ | 9377.2 |
| Eccentricity | 0.093 | 0.0151 |
| Inclination, deg | 1.849 | 1.082 |
| Mean sidereal period, day | 686.98 | 0.318910 |
| Obliquity to orbit, deg | 25.19 | Tidally locked |
| *Planetary parameters* | | |
| Mass, kg | $6.4185 \times 10^{23}$ | $1.08 \times 10^{16}$ |
| $\mu$, km/s$^2$ | $4.28283 \times 10^4$ | $7.1 \times 10^{-4}$ |
| Mean radius, km | 3389.9 | (11.32) |
| $J_2$ | 0.00196045 | (0.10053) |
| Ellipsoidal axes, km | | |
| Major | | 13.1 |
| Intermediate | | 11.1 |
| Minor | | 9.3 |

The nonspherical gravitational potential of Phobos also poses a challenge. Phobos is very irregular in shape, so that the higher-order terms of its gravitational potential are very important at short distances from the moon, possibly making the motion unstable in that region.

Another source of difficulty is the eccentricity of the Phobos orbit around Mars. It causes the force environment to change periodically in time. An S/C orbiting Phobos experiences a perturbation with the period of the Phobos orbit around Mars. This lowers the chances of the QSO being sufficiently stable. The eccentricity of the Phobos orbit, although not large, is, in fact, one of the most important parameters influencing the results and cannot be ignored. Selected Phobos and Mars parameters can be reviewed in Table 1.

## III. Review of Quasi-Satellite Orbits

### A. Origin

#### 1. *Point of View of the Three-Body Problem*

QSOs of an S/C going around Phobos are best understood using the three-body problem approach. The mass of Phobos cannot be neglected because it clearly changes the trajectory of an S/C in its vicinity. Orbiting Phobos thus corresponds to orbiting the second

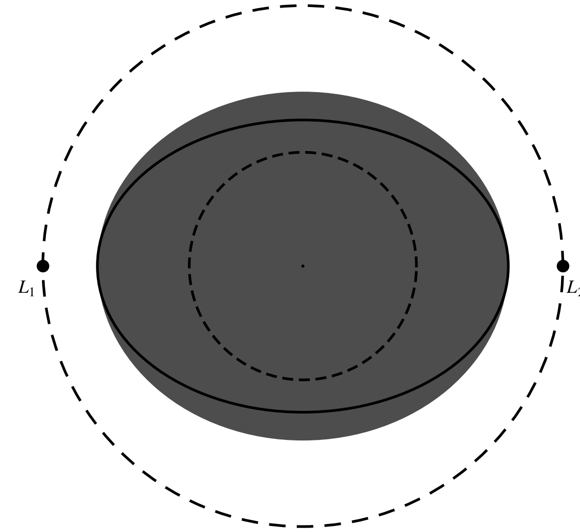


**Fig. 1 Sketch of the ellipsoid representing Phobos as viewed from the North Pole looking down on the equator. The minor axis is presented as a solid line. The interior and exterior dashed lines are, respectively, the region of influence and the Hill sphere containing the Lagrange points $L_1$ and $L_2$.**

primary, whereas Mars constitutes the first primary. However, because the mass of Phobos is very small, its region of influence lies completely below its surface and the Lagrange points $L_{1,2}$ are only immediately above it (see Fig. 1). Keplerian-type orbits around Phobos, similar to what is possible around larger bodies, are consequently impossible.

It is, however, still possible to find trajectories that circumnavigate Phobos, although they remain above the Lagrange points. They can be quasi-stable, stable, or even periodic depending on the actual conditions and the type of approximation used in each case. These are the orbits designated by QSO (or one of the alternative names referred to in the Introduction). They were identified long ago in the context of the three-body problem, in studies that can be tracked back to as early as Hill. The problem, denominated the Hill problem, arises from considering the limiting case of when the mass parameter $\mu$ vanishes, by scaling the working space dimensions by the factor of $\mu^{1/3}$ [12].

Several asteroids in the solar system are in a QSO relative to the sun and a planet. An example is the asteroid 2002 $VE_{68}$, which circumnavigates Venus [13]. There are also a few known cases of asteroids around the Earth and, in principle, such orbits could also exist in the outer solar system [14]. To the authors' knowledge, however, no such case is known.

The period of QSOs around Phobos tend asymptotically to the period of Phobos around Mars as the distance to Phobos grows [15]. For this reason, QSOs are sometimes designated quasi synchronous. At large distances QSOs can be described as elliptical orbits around Mars that remain near Phobos because they have the same orbital period (1:1 resonance). The period decreases with the distance to Phobos when its gravity, including the higher-order terms, starts to become more and more important. The eccentricity of the orbit of Phobos is large enough so that one can expect sufficiently stable QSOs at roughly the distances at which the period of the QSOs resonates with the orbital period of Phobos (2:1, 3:2, 4:3, etc.; see [15]).

### 2. *Basic Description*

To discuss the orbits in general we can use the case of QSOs around Phobos as an illustration example, because most QSOs exhibit similar qualitative geometric characteristics and this case does not present any restrictive special features such as zero eccentricity. QSOs are best perceived in the synodic, or local-vertical–local-horizontal, reference frame that rotates with Phobos around Mars. The origin of this reference frame is located at the center of Phobos and the $x$ axis always points in the direction of Mars–Phobos. The $z$ axis points in the direction of the angular momentum and the $y$ axis completes the orthogonal right-handed system. In that way, the $x$–$y$ plane coincides with the orbital plane of Phobos. In this frame the S/C performs a retrograde motion in elliptical epicycles around Phobos. These epicycles can slowly drift back and forth in the direction of the orbital motion of the moon, as depicted in Fig. 2. The guiding center of the epicycles can actually drift in any direction, but the effect is usually much more pronounced in the $y$ direction. The restoring force of Phobos makes all the difference between a probe orbiting Phobos or drifting away from it and/or being in danger of a crash. See Fig. 2 for a comparison of trajectories with and without Phobos's gravity taken into account. (Note that, depending on initial conditions, some orbits not subject to Phobos's gravity would look similar to QSOs, just like some QSOs will destabilize and drift away. The important point is that Phobos's gravity must be taken into account and will generally tend to stabilize the motion around it.) In the case of stable motion these epicycles continue to drift back and forth indefinitely. In practice, however, the perturbations forces present will cause the probe to eventually drift away. From the practical point of view it is enough that stability is assured for a sufficiently long period of time. A 3-D QSO can also be described as a drifting epicycle around Phobos but with a certain inclination relative to the orbital plane of Phobos. There are natural parameters for describing the motion arising from theoretical considerations.

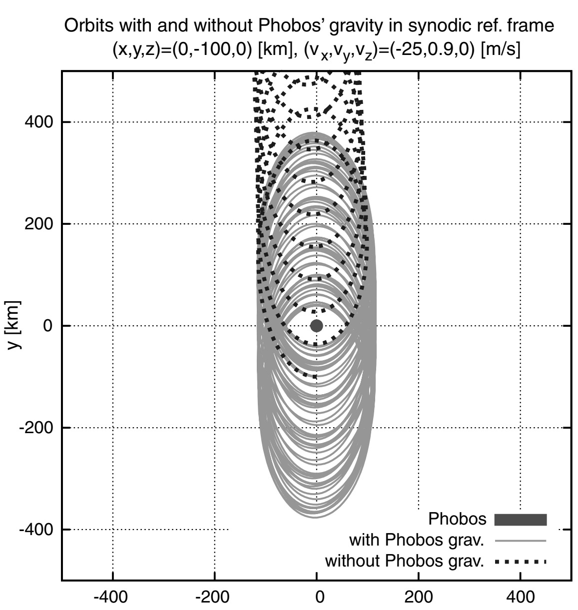


**Fig. 2 Comparison of two S/C orbits around Mars in the synodic reference frame with Phobos's gravity neglected and Phobos's gravity taken into consideration. Whereas the first (dashed line) drifts away, the latter (solid line) drifts back and forth around Phobos.**

## B. Theoretical Considerations

### 1. *Early Studies*

Analytical studies and numerical simulations have been developed throughout the last decades and sufficiently stable QSOs have been identified in several contexts, as, for example, in the restricted three-body problem (see, e.g., Hénon [16] and Benest [3,17–20], with the QSOs corresponding to the family $f$ of solutions). These early studies focused on small values of $\mu$ and on QSOs in the orbital plane of the primaries, corresponding to the $x$–$y$ synodic plane (2-D problem). The QSO can also be seen as an orbit around the more massive body and perturbed by the less massive one in a way that forces the probe to stay in its vicinity, at least for a certain period of time. QSOs are a particular type of the denominated DSOs, together with the so-called horseshoe and tadpole types of orbits [21]. They share some features and can be studied in a similar way [22].

In some cases, a horseshoe orbit can be transformed into a QSO very easily. This transition is expected to happen with the near Earth asteroid 2002 $AA_{29}$ [23].

### 2. *Perturbation Theories*

The dynamics of the QSO and its approximate long-term analysis can be best understood using first-order perturbation methods and averaging techniques [4,6,24], at least in the not-unusual case of $\mu$, $e$ being sufficiently small. In this case, the integration constants of the approximate averaged equations become the parameters defining the geometry (see Fig. 3), the position and orientation of the QSO epicycles, and their secular evolution, at least approximately. They grasp the basic 3-D geometry of the problem and provide approximate quantitative results, including the prediction of critical inclination values (maximum $\gamma$ in Fig. 3). Although these methods provide great insight into the problem, the simplifying assumptions, for instance, the assumption of circular motion of the second primary, are too severe for a direct application to the Phobos case, at least when precise results are required, that is, when the safety of an S/C is at stake.

An effort to surpass the limitations of these methods was made by applying the Lie perturbation method to the problem [5,25]. The approximate perturbed equations that describe the evolution of the slow variables are determined up to the third order to include all aspects of the problem that influence the results significantly. This approach requires a succession of canonical transformations to

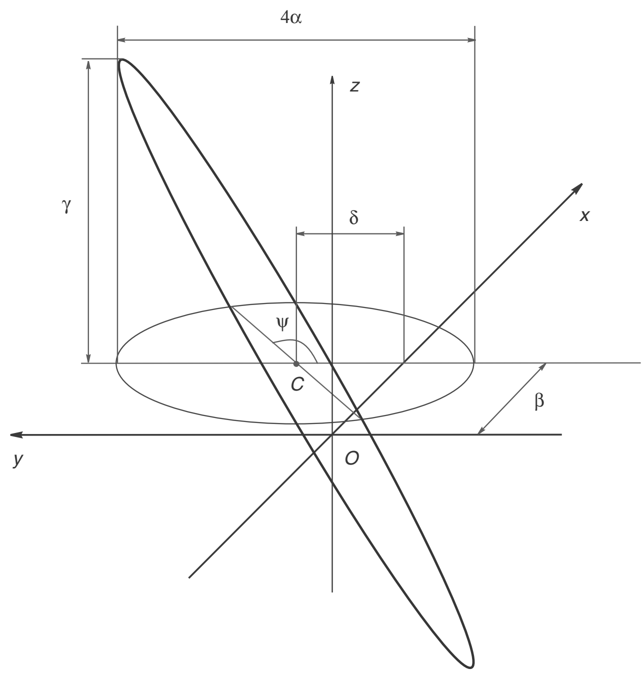


**Fig. 3 Three-dimensional geometry of a QSO as seen from the synodic reference frame *Oxyz*. The parameters $\alpha, \beta, \gamma, \delta$, and $\psi$ act as integration constants of the averaged perturbed equations [6]. The depicted epicycle has $\gamma \neq 0$ inclination, that is, goes outside Phobos's orbital (*x*–*y*) plane, where its projection and guiding center *C* are visible.**

reduce the equations to a form required by the Lie method. The complicated nature of the procedure necessary to reach the required precision leads to the use of an averaging scheme, using the $e = 0$ and unperturbed Keplerian orbits as starting point. These difficulties are mainly due to the huge difference in the orders of magnitude of the parameters of the problem in the case of Phobos, implying the original theory to be of restricted usefulness. Nevertheless, achieved agreement with the numerical simulations was up to 10–20%, but only with higher-order gravitation terms not taken into account in the simulations and restricting them to QSOs not going significantly out of the orbital plane of Phobos. The high complexity of the Lie method, with cumbersome procedures required for application to more practical cases and the difficulty of grasping its physical concepts, suggests that a search for alternative perturbation theories must be performed in the future.

*3. Theoretical-Numerical Approach*

There are also some numerical or hybrid approaches to the problem, including some applied specifically to the case of QSOs around Phobos and Deimos [15]. These are some of the best-known and most interesting examples. The study referred to was restricted to the orbital plane of Phobos but including $e \neq 0$ and Mars oblateness. It also used an ellipsoidal model for the moons of Mars to increase the similarity with the real problem. The zero-eccentricity model yielded insight into the problem and was used as a stepping stone for more complex cases, from periodic orbits at any distance from Phobos with $e = 0$ to resonant orbits and nonperiodic orbits with $e \neq 0$. The Floquet theory was used, after a periodic orbit had been found, to determine the Poincaré exponents and conditions of sufficient stability and instability. A small numerical exploration of the phase space was performed using epicycles starting only from the *x* axis, used as a kind of Poincaré section, and with simulations always starting at perimartem. With a 25-day criterium for sufficient stability, it was determined that the velocity of the probe had to have a precision of 10 cm/s or better, if the injection maneuver was performed at the *x* axis, to establish stable orbits.

A global numerical search for periodic orbits that included stability analysis was also developed for the case of the Jupiter–Europa system, including a search for three-dimensional solutions [26]. The resulting database of distant satellite orbits included many from the DRO (or QSO) family and is a practical reference for the preliminary design of missions to Europa.

*4. Alternative Approaches*

Other approaches to the problem include considering orbits of the S/C around Mars, with Phobos acting as a perturbation [27]. Results are similar to the ones of the already-discussed equivalent approach of first-order perturbations, at least for rendezvous orbits, and with the same limitations. There are also other studies in the more general context of coorbiting objects. They consider several families of orbits, namely, QSO, horseshoe, and tadpole orbits, that share some common ground [22].

*5. Recent Developments*

Recently there has been some work using some more modern methods, for example, the manifold theory, to study the general problem of distant satellite orbits in the context of the circular restricted three-body problem [28] (CR3BP), with emphasis on the transfer (namely, in the case of the Earth–moon system).

There has been also the proposal of a heuristic method to estimate the qualitative stability of real-world distant orbits, including QSOs, using fast Lyapunov indicator (FLI) maps in the CR3BP [29–31]. The idea is that trajectories robust enough to small perturbations in the simplified problem may correspond to long-term stability in real problems. Application to the Jupiter–Europa system was developed as example. This technique is very promising in the initial classification and assessment of QSOs stability.

## C. Quasi-Satellite Orbit Features

It is worthwhile to review the main features of QSOs to have a broad sense of the problem. From the synodic reference frame point of view, they are elliptic epicycles for which the center, the guiding center, slowly drifts mainly back and forth in the *y* direction. In cases other than the Phobos case, in which the parameters of the problem are different, the elliptical epicycles can be largely distorted and the drift of the center can become a sensible 2-D motion [17].

The ratio between the major and minor axes of the epicycles is about two. The major axis lies in the general direction of the orbit. The speed of the S/C along the epicycle seems to vary accordingly,

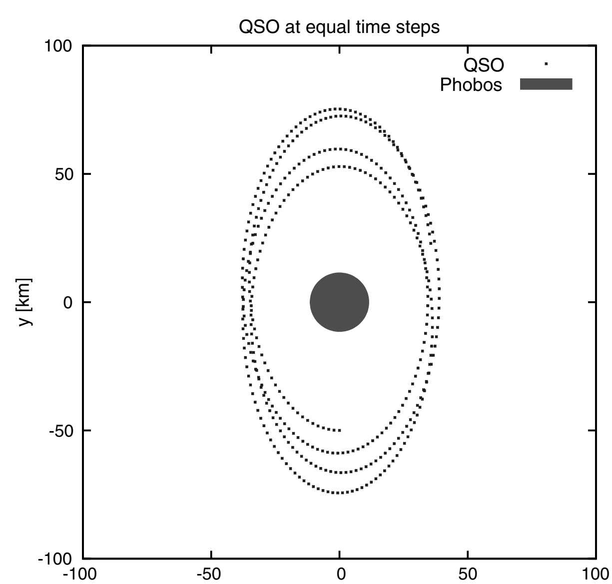


**Fig. 4 Geometry of a QSO around Phobos lying in the orbital plane of the former ($\delta = 0$), plotted at equal time steps and seen from the synodic reference frame in which Mars is in the direction of the negative *x* axis. The elliptical epicycle, with an axes ratio approximately equal to two, drifts back and forth in the *y* direction. The motion is retrograde.**

with its value at the $x$ axis being about twice the value at the $y$ axis (see Fig. 4).

In the case of the restricted three-body approximation, the period of the QSO can be chosen at will, meaning that there are stable solutions at all increasing distances from the moon. The orbital period increases with increasing distance to the moon. It asymptotically approaches the orbital anomalistic period of the moon until, when sufficiently far away, the orbit of the S/C is best described as being around the planet. When the eccentricity of the orbit of the moon cannot be neglected, which is the case of Phobos, the period must be a multiple of the orbital anomalistic period of Phobos. In the case of quasi-stable orbits, the exponents describing the instability can be quite small and instabilities can take a long time to grow, meaning that these sufficiently stable QSOs can eventually be used safely as parking orbits. The geometry of the QSOs, and its evolution, is much more complicated in the 3-D case. It is nevertheless possible to foresee the approximate value of the critical relative inclination $\gamma/\alpha$ (see Fig. 3) beyond which a sufficiently stable 3-D QSO cannot survive. This critical value can be small [4].

The complexity of the behavior of the QSO can be seen clearly in the Mars-centered inertial reference frame. In Fig. 5, the orbital elements $a$ (Fig. 5a) and $e$ (Fig. 5b) of an S/C in a QSO and Pbobos with respect to Mars are plotted over a time span of five days. The elements of an S/C with the same initial conditions but not subject to the influence of Phobos are also plotted for comparison. The selected QSO lies in the Phobos orbital plane and has average dimensions of (103 km × 62 km). This is sufficiently small for the higher-order gravitational terms of Phobos to be important, even if indirectly. These terms are responsible for the periodic variation of the orbital elements of Phobos, which can be easily checked by integrating the equations of motion considering Phobos as a point mass. This variation will influence the motion of a sufficiently closed S/C. It has a period of about a quarter of a day, different from the orbital period of Phobos (about a third of a day; see Table 1). The irregularities of the S/C elements at their extreme values (see Fig. 5) are probably due to the eccentricity of the orbit of Phobos and the evolution of the orbital elements of Phobos discussed earlier. This behavior is amplified by the fact that the present simulations did not start at perimartem. The S/C elements without the effect of Phobos taken into account are simply Keplerian-like, that is, describing simple elliptical orbits, which demonstrates that Phobos is responsible for the complex behavior described. The higher-order terms of the Mars potential have little influence, at least on the qualitative behavior of the S/C, which is an expected result because Mars is too far away and the simulations did not last long enough for Mars's gravitational perturbations to be noticeable. Similar results could be obtained for the argument of perimartem and the true anomaly.

### D. Practical Quasi-Satellite Orbits Around Phobos

#### 1. *Rationale*

Several approaches were used in the literature to study QSOs: the full numerical integration of the problem, the three-body problem approach using perturbation methods and semi/analytical procedures, and Keplerian motion around Mars with Phobos considered as a perturbation.

In the case of QSOs around Phobos, the values of the parameters (see Table 1) relevant to the problem make it difficult to study the problem theoretically. The formulation becomes too complex and the necessary approximations that would make the calculations accurate enough too severe. From the practical point of view, it is necessary to take into account all the parameters that can influence the outcome, because a wrong forecast can entail losing the mission. In the case of Phobos, the moon is highly irregular and higher-order gravitational terms will play a role that cannot be neglected, especially in the most interesting case of smaller QSOs. In the end, it will be always necessary to use a numerical procedure, simulating the actual conditions. The problem is too complex to rely solely on any type of theoretical approximation.

#### 2. *Phobos–Grunt Procedure*

The approach of the Phobos–Grunt mission [8–11] was to use theoretical calculations to gain preliminary insight into the problem and then to proceed numerically to find precise results. Only the planar case was considered at first, and no higher-order gravitational terms were taken into account. The parameters $e$ and $\mu$ were set to zero and the equations were linearized to get the analytical zeroth-order solution. Subsequently, a phase space scan was performed to investigate the general behavior of the QSO and select the most suitable candidates. These theoretical simplified solutions were checked afterward against the full numerical model.

A classification scheme was used to categorize the orbits into families [9]. The maximum amplitude of the epicycles in the $x$ and $y$ directions in the synodic reference frame were used as a classification criteria, as well as the length of the dense regions provoked by the passage of consecutive epicycles as they drift, in the negative and positive sides of the $x$ and $y$ axes. The number of revolutions per orbital period of Phobos was used as well.

The Phobos–Grunt approach is well balanced between the simpler, faster, and more insightful theoretical approach, which is insufficient by itself, and the full numerical procedure.

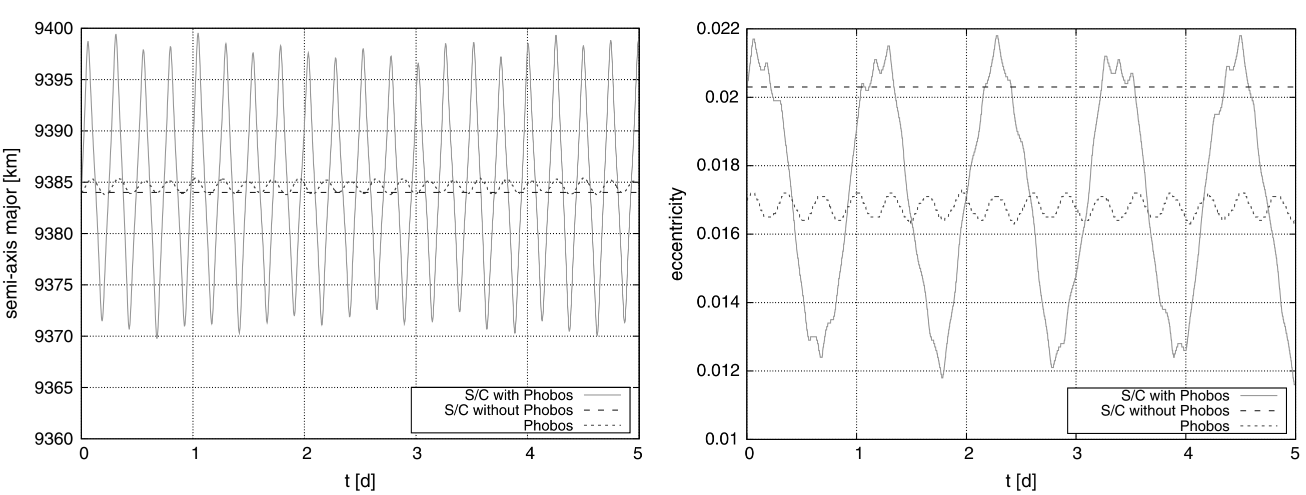


**a) Semimajor axis** **b) Eccentricity**

**Fig. 5 Semimajor axis and eccentricity, with respect to Mars, of Phobos and an S/C. The largest variation of both orbital elements happens in the case of an S/C subject to Phobos's gravity, a 103 × 62 km QSO in the orbital plane of Phobos, and its irregularity reflects the complexity of the situation. The observed periodic variations of the orbital elements of Phobos are mainly due to non-Keplerian gravitational interactions between Mars and Phobos. If Phobos did not exist, an S/C would have a simple Keplerian-type orbit around Mars (represented by the straight line in both cases).**

## IV. Simulations of Quasi-Satellite Orbits Around Phobos

### A. Objectives of Present Approach

This work is a preliminary assessment of the required conditions for orbiting Phobos in a QSO. The goal was not only to gain experience and develop capabilities in dealing with this type of problem, as well as getting used to its features and difficulties, but also to address certain specific mission-design-related questions such as eclipse durations and occultation occurrences.

A numerical approach was chosen for several reasons. First, it made it possible to obtain initial results sufficient for a rapid preliminary assessment. Second, numerical simulations with real ephemerides allowed the inclusion of all relevant perturbations and, thus, gave confidence in the obtained results for practical applications. Third, the numerical approach made it possible to explore the 3-D case, which would be difficult and time consuming to explore theoretically at this stage. An approach similar to the Phobos–Grunt approach, possibly together with the use of FLI maps, which combines theoretical considerations with numerical simulations, should be adopted for more systematic and thorough searches because theoretical insights can lead to a faster and better assessment of the results.

### B. Issues to Address

The following issues are addressed in this study: How can sufficiently stable QSOs around Phobos be attained? What is the sensitivity of the orbit stability to the initial conditions? What are the main features of the attained QSOs, and what is their degree of suitability to a sample return mission?

In the framework of the latter question, eclipses, Earth occultation times, and the ground track on Phobos (using the spherical approximation of Phobos) were calculated. In addition, the illumination of the ground track by the sun was also determined, as this influences the observation conditions.

Because this study is not yet as systematic as the one already conducted for the Phobos–Grunt mission, a simplified version of their classification scheme was adopted to categorize the QSOs. The classification criteria are the average $x$ and $y$ dimensions, together with the additional average $z$ dimension to allow 3-D QSO analysis, as well as the average period of revolution in the synodic reference frame.

### C. Calculation Setup

A software package was developed that numerically integrates the equations of motion of an S/C in the vicinity of Phobos, taking into account all major perturbation forces, including Mars's and Phobos's higher-order gravity terms, solar radiation pressure, and the sun's gravitation. We integrated the equations of motion using an eighth-order Runge–Kutta algorithm with a time step of 10 s, which provided an adequate equilibrium between accuracy and the duration of the simulations. Testing showed that an integration time step of 1 s resulted in relative variations smaller than $10^{-4}$ in the results at the end of a 100-day simulation of a sufficiently stable orbit. Because the effect of Mars on the S/C is significant, the use of a different gravity model of Mars for determining the motion of the S/C (first few terms of the potential expansion) than for determining the motion of Phobos (a standard routine based on ephemeris determined by observation and so including all the forces) could introduce a spurious relative behavior of the S/C with respect to Phobos. To avoid it, the motion of Phobos is also determined by integration of the equations of motion together with the motion of the S/C, using the same force model.

Because the QSOs investigated in this work are supposed to be used for observation and as a stepping stone to land on Phobos, they do not need to be stable in the strict sense, that is to say, forever. A quasi-stable orbit, which drifts away only after a long time, can be used as well. A stability analysis determined that the only Poincaré exponents that can lead to unstable orbits were found to be too small for one to have confidence in the obtained result relative to the type of orbit (stable or unstable). But even if the resulting orbits are found to be unstable, the smallness of the Poincaré exponents module assures that the instability will take a long time to grow providing sufficient stability [15].

In this work, we typically simulate the orbits for 30 days and consider them stable enough if no crash occurs and if they do not surpass the maximum distance of Phobos of 1000 km during that time. Other simulations in literature use about the same time limit (100 revolutions in [9], 25 days in [15]). It offers enough time for a probe to recover from a problem if something goes wrong. Other than in the uninteresting case of QSOs so large that the limit of 1000 km is achieved in the drift of the epicycle, it is extremely improbable that a probe will remain in the vicinity of Phobos if the considered upper limit is reached.

Results show that most unstable orbits reach the bounds very rapidly, usually after a few days. At the same time, a particular quasi-stable QSO was simulated for up to 500 days without losing its stability.

The various cases discussed here do not constitute a systematic search of the phase space. The goal was to test the difficulty of finding sufficiently stable solutions under real conditions, that is, using the real values of the parameters of the problem rather than studying idealized cases. To achieve this goal, we focused on special promising zones of the phase space. Thinking about the problem in the synodic reference frame, all QSOs must go around the $z$ axis. Thus, we first examined what happens in the plane perpendicular to this axis in an approach resembling the Poincaré section method. This was used before [15] in a more limited way because calculations were restricted to QSOs in the orbital plane of Phobos, only initial velocities perpendicular to the direction Phobos–S/C were considered, and the initial positions were limited to the $x$ axis.

We started by keeping the initial position constant with $z = 0$ and varying all the components of the initial velocity. From the mission analysis point of view, the option of performing an insertion maneuver somewhere on the $y$ axis seems as good as on the $x$ axis and, as we will see, there could be some advantages. In a second step, we varied the $y$ component of the initial position and $v_x$ of the initial velocity, while keeping all the remaining components of the position and velocity zero, starting from a quasi-stable solution found in the first scan. We reasoned that this approach would find sufficiently stable solutions with various dimensions easily. We started with the better-known 2-D problem, simpler to study, before generalizing to the 3-D case. Note, however, that even with the initial conditions limited to the $x$–$y$ plane, the orbit does slowly build up components in the $z$ direction due to the three-dimensional forces acting on it.

The 3-D case can be easily set up in two ways: a QSO starting on the $x$–$y$ plane with a nonzero $z$ component of the velocity will extend substantially into the $z$ direction, with the "node line," the intersection between the plane of the instantaneous epicycle and the $x$–$y$ plane, perpendicular to the direction of Mars; alternatively, we can move the initial position from the $x$–$y$ plane along the $z$ direction, trying to put the "node line" toward Mars.

Although we did not perform a full phase space scan, the QSOs found do provide an overview of what can happen in the general 3-D case.

In this preliminary study, no special attention was given to how Phobos's orbit, and, hence the QSO, is oriented relatively to the sun or Earth. The epoch used was chosen by a possible date selected for the mission to arrive to Mars, and it was set to March 2017. At this time, the declination of the sun relative to Phobos orbital plane is around $-9°$, so that the orbital plane of Phobos is almost sideways to the sun.

## V. Search for Sufficiently Stable Quasi-Satellite Orbits Around Phobos

### A. Varied Initial Velocity Starting at the Same Position

#### 1. Scanning the Phase Space

To assess the difficulty of finding a sufficiently stable QSO around Phobos, we began our search by setting the S/C on the fixed point $(x, y, z) = (0, -100\ \text{km}, 0)$ in the synodic reference frame and propagating its trajectory forward for just one day (roughly three orbital revolutions of Phobos around Mars) with varied initial velocities. After a first improvement of the mesh, when it had become obvious that the velocity component $v_y$ has to vary much less than the other components, a scan of $9^3 = 729$ simulations was performed in which the components $v_x$ and $v_z$ of the initial velocity ranged from $-40$ to 40 m/s, whereas $v_y$ ranged from $-4$ to 4 m/s.

The results are shown in Fig. 6, in which we use a two-part figure to display the information. The figure parts show the maximum and minimum altitudes relative to Phobos reached by the S/C after one day of propagation (upper pane) and the value of the three initial velocity components (lower pane) for each performed simulation. Each horizontal position, therefore, represents an individual simulation defined by a specific combination of initial velocity components, indicated in the lower pane, that resulted in a certain maximum and minimum altitudes reached during the simulation, shown in the upper pane. The three initial velocity components vary within the defined domain along the simulation number. However, each component needing to be reset periodically leads to adjacent points in the figure not necessarily being adjacent in phase space. Therefore, the results in the upper pane are sometimes discontinuous. Presenting the results in this form, however, has the advantage of allowing the display of more information for each simulation over a larger domain, which in turn enhances the visualization and possible identification of the dependence of the results on the initial conditions.

Most of the shown orbits will prove to be unstable when the propagation is prolonged to 30 days. Nevertheless, it is instructive to examine the plot at this time to detect general trends. The S/C appears to have a high probability of not escaping from Phobos for small initial velocities in the $y$ direction, that is to say, in the region $v_y \in [-2, 2]$ (m/s). However, for negative values of $v_y$ in this range, the likelihood of a crash seems to increase. At the same time, a high absolute value of the $v_x$ component increases the maximum altitude reached. For $v_x \approx 0$, a crash seems guaranteed. An increase in inclination, that is to say, $v_z \neq 0$, appears to lower the probability of a crash again.

Plotting the simulation results in a different order makes some of the aforementioned findings even more obvious. Figure 7 shows the same simulation as Fig. 6 but with the velocity variations performed in a different order. Now $v_x$ is the last to vary and $v_y$ the first. The correlation between the likelihood of escape and the value of the $v_y$ is now even more pronounced by the high-frequency periodic variation of the maximum altitude curve. The bowl shape of its enveloping curve, on the other hand, is again due to the tendency toward escape for large absolute values of $v_x$ on the sides of the axis and toward crashes for small values of $v_x$ in the middle.

To assess the real stability of the QSOs, it is necessary to continue the simulation for much longer. After seven days of simulation, most of the depicted QSOs in Fig. 6 have crashed on Phobos or exceeded the maximum altitude limit of 1000 km that we set. After 30 days, only a few remain, as shown in Fig. 8. A refinement of the simulation by narrowing the intervals of the velocity components can now focus on the regions in which sufficiently stable orbits seem to occur.

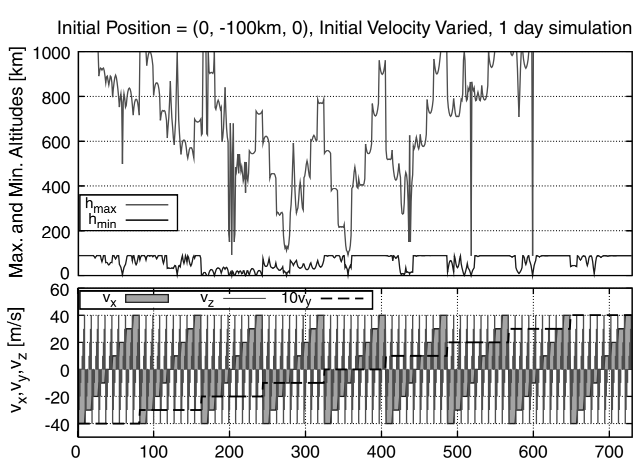


**Fig. 6 Maximum and minimum altitudes relative to Phobos, after one day of simulation, of an S/C placed at $(0, -100\ \mathrm{km}, 0)$ in the synodic reference frame (upper pane), for each set of values of the components of the initial velocity (lower pane).**

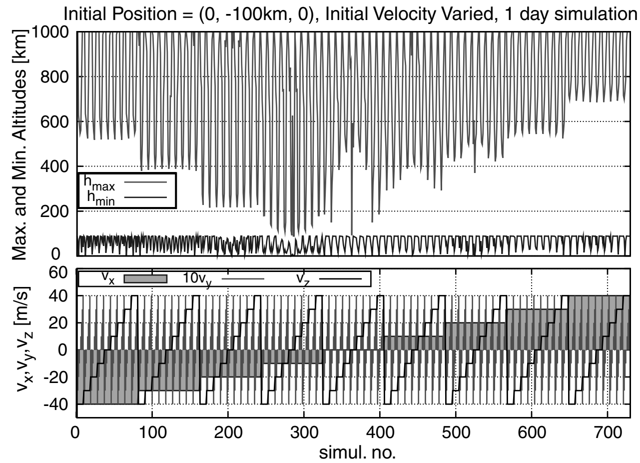


**Fig. 7 Same as Fig. 6 but with the order of the simulations changed in a way that, from each simulation to the next, $v_y$ is the first to vary and $v_x$ the last. The variation due to $v_y$ clearly dominates. The influence of the other components are also detected in the smother variations of the maximum reached altitude.**

### 2. *Refined Simulations*

A new set of $9 \times 16 \times 9 = 1296$ simulations scans the narrower regions $v_x \in [-32, -16]$ (m/s), $v_y \in [-1, 0.5]$ (m/s), and $v_z \in [-8, 8]$ (m/s) in which sufficiently stable QSOs seem to exist. The velocity components are $(v_x, v_y, v_z) = (-32 + 2i, 0.1j, 2k)$ (m/s) with $i$, $j$, $k$ integers in the intervals $i \in [0, 8]$, $j \in [-10, 5]$, and $k \in [-4, 4]$. The duration of the simulations is, as before, 30 days or until a stop condition is reached.

The results are shown in Fig. 9. Having limited $v_y$ to the region $v_y \in [-1, 0.5]$ (m/s), hardly any crashes occur anymore. The S/C still escapes at the extremes of this interval, but otherwise the QSOs are stable over this time interval. The maximum altitude clearly increases with increasing negative $v_x$ component, whereas the variations in $v_z$ only lead to small variations in the maximum and minimum altitudes.

At the extremes of the interval, however, a nonzero $v_z$ is what makes the QSO unstable. Figure 10 offers a more-detailed version of Fig. 9, emphasizing this correlation.

### 3. *Discussion of Results*

For these QSOs, the $v_x$ component needs to be negative, preferably around $v_x = -20$ m/s. This has an obvious explanation: because the

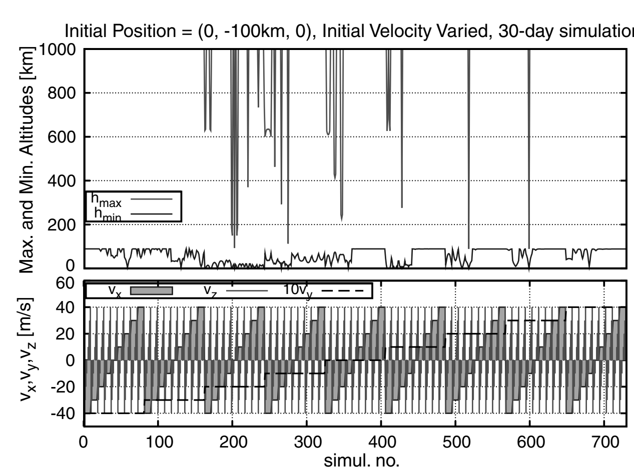


**Fig. 8 Same as Fig. 6 but for 30 days of simulation. Most solutions were proven unstable, but a few remained, indicating possible regions of (sufficient) stability.**

synodic reference frame rotates with the motion of Phobos around Mars, a zero inertial velocity toward Mars on the $y$ axis entails a negative $v_x^{\text{rot}}$ component induced by the rotation of the reference frame. At the point chosen for these simulations, it has the value

$$\mathbf{r} = (x, y, z) = (0, 100\ \text{km}, 0) \Rightarrow v_x^{\text{rot}} = (\boldsymbol{\omega} \times \mathbf{r})_x = -22.8\ \text{m/s} \quad (1)$$

inducing the observed shift of the stable $v_x$ values. This is interesting information to take into account when searching for sufficiently stable QSOs at different distances from Phobos, as the shift depends linearly on the distance.

The most critical velocity component for stability is $v_y$, that is, the velocity component toward the center of the epicycle. This confirms the findings of Wiesel [15] (although he used a different Poincaré section) with a small difference: the interval in which $v_y$ must be contained is about 1 m/s larger than the 10 cm/s range obtained in [15]. This can be due to a different selection of the phase space but can have another explanation as well: because the epicycles drift along the $y$ axis, it is possible that different $v_y$ values lead to the same QSO but at different moments of its drifting motion. It is, however, not obvious at this time what will be the exact impact of this aspect on the insertion into a QSO. This issue should be clarified in the future because, if true, there could be a clear advantage to performing insertion maneuvers into a QSO on the $y$ axis instead of on the $x$ axis because the precision requirement for the velocity would be lower here.

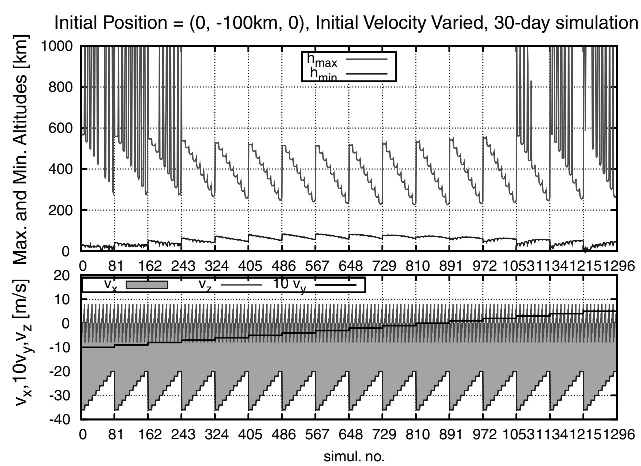


**Fig. 9 Same as Fig. 6 but for 30 days of simulation and a finer mesh, concentrated on one possible sufficiently stable zone. There are clearly many sufficiently stable solutions in this range. The variation of the minimum and, especially, the maximum altitudes are strongly correlated with the variation of the velocity components.**

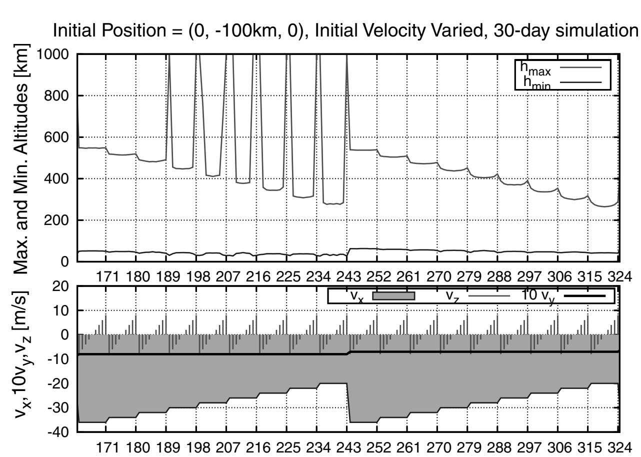


**Fig. 10 Detail of Fig. 9 in which the correlation between the minimum and the maximum altitudes with the velocity components can be better observed.**

Apart from $v_y$, the other velocity components can vary by a few meters per second, $v_x$ a little more than $v_z$, without the QSO losing stability in the time span considered. The tighter restriction on $v_z$ is possibly due to reaching the critical inclination when the restoring force is not enough to maintain the epicycle [27].

Note that the dimensions of these QSOs are smaller than it seems from the maximum altitude values. Because of the drift of the epicycle, the maximum altitude is usually reached at more or less the same epicycle as the minimum altitude and this should happen in the overall $y$ direction (the direction of the major axis of the epicycle; see Fig. 4) Hence, the major axis of a stable epicycle (see Fig. 3) is approximately

$$4\alpha \sim h_{\max} + h_{\min} + 2R_{\text{Ph}} \quad (2)$$

### B. Varied Distance and Speed in the *x–y* Plane

#### 1. *Setting up the Simulations*

Having found sufficiently stable QSOs at a fixed initial position and with varied initial velocities, we searched for sufficiently stable QSOs of different sizes by varying the initial distance from Phobos starting from the previous initial position and varying the velocity component that we expect should change to achieve quasi-stability, while maintaining the other velocity components at values that previously resulted in sufficiently stable QSOs. We varied the distance along the $y$ axis from $-95$ to $-15$ km, and $v_x$ from $-15$ to $-8$ m/s. $y = -15$ km corresponds to the S/C being only a few kilometers above the Phobos surface. All other position and velocity components were set to zero because these values seem to be good candidates to achieve sufficient stability. The range of $v_x$ values was lower than before, due to the shorter distances to Phobos and the therefore smaller effect of the rotational velocity of the synodic reference frame (see previous section). The duration of each simulation was again 30 days or until the S/C either crashed on the Phobos surface or reached an altitude of 1000 km or greater.

The results are depicted in Fig. 11, in which again the maximum and minimum reached altitudes are plotted against each different position and velocity combination. There are clearly many sufficiently stable QSOs in the examined range. From Fig. 12, which is a more-detailed version of Fig. 11, it can be seen that even with an initial position very close to Phobos it is possible to enter into sufficiently stable QSOs.

We defined an epicycle (anomalistic) period as the time between consecutive attainment of the maximum value on the $x$ axis, which roughly coincides with one of the axes of the elliptical epicycle. Figure 11 shows the average period of an epicycle for each initial position and velocity combination. Without more-detailed information, these values are only meaningful for QSOs that are still stable at the end of the 30-day simulation.

#### 2. *Discussion of Results*

Figure 11 shows that, when the initial $y$ position increases, that is, the initial altitude diminishes, the minimum altitude reached while orbiting Phobos in a QSO becomes smaller and the maximum altitude larger. At the same time, the average dimensions of both $x$ and $y$ of the epicycles (not shown in the figures) tend to become smaller. This suggests that, for equal velocities, the drift of the epicycles increases with decreasing initial altitude while their overall size decreases.

The duration of the average epicycle period also decreases with an increase in the proximity to Phobos. This confirms the results obtained in [15]. The effect becomes more pronounced with a simultaneous increase in the initial velocity $v_x$. The latter also leads to a decrease of the maximum and minimum altitudes. The effect is more pronounced in the maximum altitude, implying that the QSOs become rounder, with the elliptical epicycles less eccentric. Sufficiently stable QSOs were found at roughly the expected resonant periods of 1:1 (farthest away), possibly 2:1 or 3:2, and 4:3

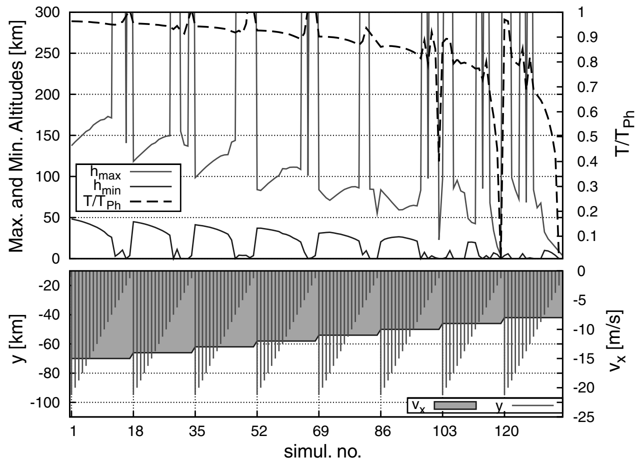


**Fig. 11 Maximum and minimum altitudes as well as the normalized period of the S/C around Phobos, obtained in a phase space scan in which the initial distance to Phobos and the initial $v_x$ component vary, while all other initial position and velocity components are zero.**

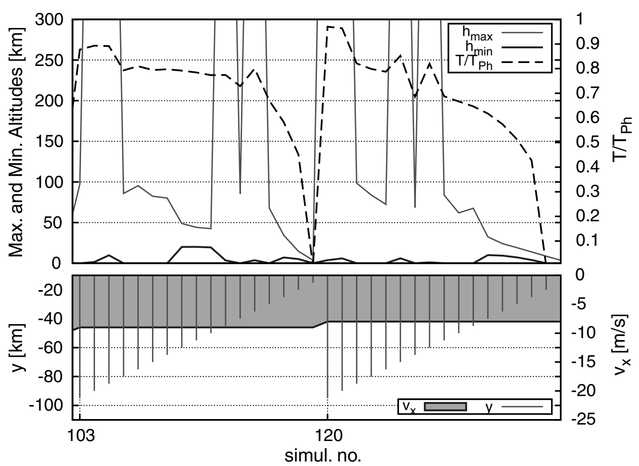


**Fig. 12 Detail of Fig. 11 clearly showing some sufficiently stable solutions near Phobos.**

(see Table 2). Values are not exactly as expected, which is probably due to the large higher-order gravity terms of Phobos.

While the epicycle drift increases and the QSOs become smaller with a decreasing initial altitude, the number of sufficiently stable QSOs found in this region is smaller than elsewhere. This could be due to the ellipsoidal shape of Phobos, that is, its large $J_2$ value (cf. Table 1). A heuristic analysis of the relative importance of the forces involved strongly suggests this. At approximately 25 km from Phobos, the $J_2$ term is comparable with the perturbation induced by the eccentricity of the Phobos orbit, and its relative importance grows faster with a decreasing distance to Phobos than all other involved forces. However, the lower number of sufficiently stable QSOs found in the part of the phase space considered here could also be a simple consequence of the fact that the more eccentric epicycles are ruled out because they crash onto the Phobos surface. In the zone near Phobos, a tighter control of the velocity components would therefore be required.

Table 2 shows some examples of the stable QSOs that were found, including one that clearly spans into the $z$ direction (see Sec. V.C). Some additional parameters are shown, such as the average dimensions of the QSO in the $x$, $y$, and $z$ directions, corresponding approximately to the parameters $4\alpha$, $2\alpha$, and $2\delta$, respectively. The average anomalistic period of each QSO, normalized by the orbital period of Phobos, is also shown. The overall trend is a decrease of the dimensions, period, and initial velocity required for stability of the QSO when Phobos is nearer. Note that, because we are solving the numerical problem, there is no perfect two-dimensional orbit. Even orbits starting in the $x$–$y$ plane with no $z$ velocity component will slightly drift outside the plane, as the $\ell_z$ dimension shown in Table 2 demonstrates.

It should be emphasized that the precision on the initial velocity required to insert a probe into a QSO can be easily met with today's technology. All the variations in the velocity are of the order of magnitude of at most 10 m/s, usually much less. Correction maneuvers will not cost much fuel. Nevertheless, the advantage of being in a sufficiently stable orbit is unquestionable, especially if something goes wrong.

### C. Quasi-Satellite Orbits Going Out of the Plane

#### 1. Test Case Definition

To search for sufficiently stable 3-D QSOs, we picked an appropriate QSO previously obtained with $y = -100$ km (see Sec. V.A) and pushed the initial position outside the $x$–$y$ plane. The resulting initial conditions $(x, y, z) = (0, -100, 40)$ [km] and $(v_x, v_y, v_z) = (-20, 0, 10)$ [m/s] lead to a QSO with a considerable initial inclination to the $x$–$y$ plane, even more accentuated by the positive initial $v_z$ component. The 3-D QSO obtained fulfilled our conditions for sufficient stability, meaning that within the first 30 days the S/C neither crashed nor escaped.

The projections of the QSO onto the $x$–$y$, $x$–$y$, and $y$–$z$ planes, as well as a three-dimensional view of the test 3-D QSO, are depicted in Fig. 13 for the first day of the simulation and in Fig. 14 for the full 30-day simulation.

Several other orbits with slightly different initial conditions were examined, but all lead to the same basic geometry and properties. Therefore, the test case defined earlier will be sufficient to illustrate the results.

#### 2. Discussion of Results

Although the effect is not visible in a one-day simulation, when longer times are considered it is easy to see that the trajectories fill a torus around Phobos, meaning that the parameter $\psi$ (cf. Figure 3) changes considerably. Geometrically, this resembles a variation of the longitude of the ascending node.

The key results are that it is relatively easy to obtain sufficiently stable 3-D QSOs and that the epicycles do not lie in a fixed plane. Operationally, this can pose a challenge, but from a mission design point of view it is advantageous with regard to the surface coverage.

**Table 2 Examples of QSOs found during the phase space search. Most are 2-D QSOs with all initial $z$ components zero. However, because we are solving a problem in the space with realistic forces, they end up extending slightly in the $z$ direction. The last entry is a 3-D QSO that will be used extensively in the text**

| Orbit | Initial conditions, km, m/s | | QSO dimensions, km | Altitude, km | | |
|---|---|---|---|---|---|---|
| Type | $(x, y, z)$ | $(v_x, v_y, v_z)$ | $(\ell_x, \ell_y, \ell_z)$ | $h_{max}$ | $h_{min}$ | $T_{anom}$[a] |
| 2-D | (0, −100, 0) | (−20, 0, 0) | 169.6, 335.3, 0.06 | 226.8 | 62.44 | 0.9850 |
| 2-D | (0, −50, 0) | (−10, 0, 0) | 72.72, 127.6, 0.12 | 64.90 | 22.80 | 0.8401 |
| 2-D | (0, −50, 0) | (−9, 0, 0) | 62.37, 103.3, 0.02 | 42.50 | 19.42 | 0.7734 |
| 2-D | (0, −35, 0) | (−8, 0, 0) | 43.79, 61.47, 0.08 | 24.08 | 9.32 | 0.5741 |
| 2-D | (0, −25, 0) | (−8, 0, 0) | 33.72, 42.02, 0.33 | 13.81 | 4.02 | 0.4270 |
| 3-D | (0, −100, 40) | (−20, 0, 10) | 168.6, 334.2, 121.4 | 256.7 | 62.84 | 0.9880 |

[a]Anomalistic period, in units of the mean sidereal period of revolution of Phobos.

The rate of change of $\psi$ can eventually be determined by approximate theories, a prediction that would be of great advantage.

The simulations performed for this study are only an initial effort toward the general study of 3-D QSOs. There will be much work needed in the future, including the help of theoretical work, to obtain educated guesses on certain crucial parameters. In particular, phase space searches must be set for a more systematic study.

## VI. Additional Mission Analysis Issues

Finding sufficiently stable QSOs is not sufficient to ensure the success of a mission. There are other factors to consider, such as the duration of eclipses and occultations of the Earth by Mars or Phobos, the ground track of the S/C on Phobos, and the illumination of the ground track point.

We used a sample QSO to examine the aforementioned features. Because one of our goals was to assess orbits not restricted to the $x$–$y$ plane, we considered once more the 3-D QSO presented in Sec. V.C as a test case. The parameters of this QSO can be found in the last entry of Table 2.

The chosen epoch for the calculations was based on a mission opportunity study. The orbital plane of Phobos is inclined approximately 25° with respect to the ecliptic at that time. Its orientation relative to the sun and the Earth changes over time.

The orientation has a high impact on the values of the quantities determined in this section. Some of the results obtained can thus vary a lot based on the epoch chosen. Additional analysis is therefore required, which examines different orientations of the orbital plane of Phobos at different times of the year.

An issue not addressed here, because it is related to the overall design of the mission, is the minimum angle between the Earth and the sun usually required by communications. This issue has an influence on the eclipse and occultation sequence and the possible time frame of the mission. For a minimum required angle of 30° for Earth–Mars–sun, there are more than 100 days of possible operation, which should not constitute a problem.

### A. Eclipses and Occultations

Figure 15 depicts the eclipse and occultation events that occur between days 21 and 23 of the simulation. This particular time span was chosen to illustrate the most complex eclipse and occultation behavior detected. The duration and periodicity of both the occultation and eclipse events are fairly regular. A few secondary eclipse events with a shorter duration can, however, appear. The latter are due to Phobos instead of Mars being between the S/C and the sun.

For other QSOs, some parameters may vary but the regularity of the eclipse and occultation events is so high that we do not anticipate any surprises. It is nevertheless possible that at a different epoch the different sun declination with respect to Phobos's orbital plane changes the duration drastically. Because QSOs tend to be resonant with the orbit of Phobos, an S/C that is inserted between Mars and Phobos, with Phobos toward the sun, could remain hidden from the

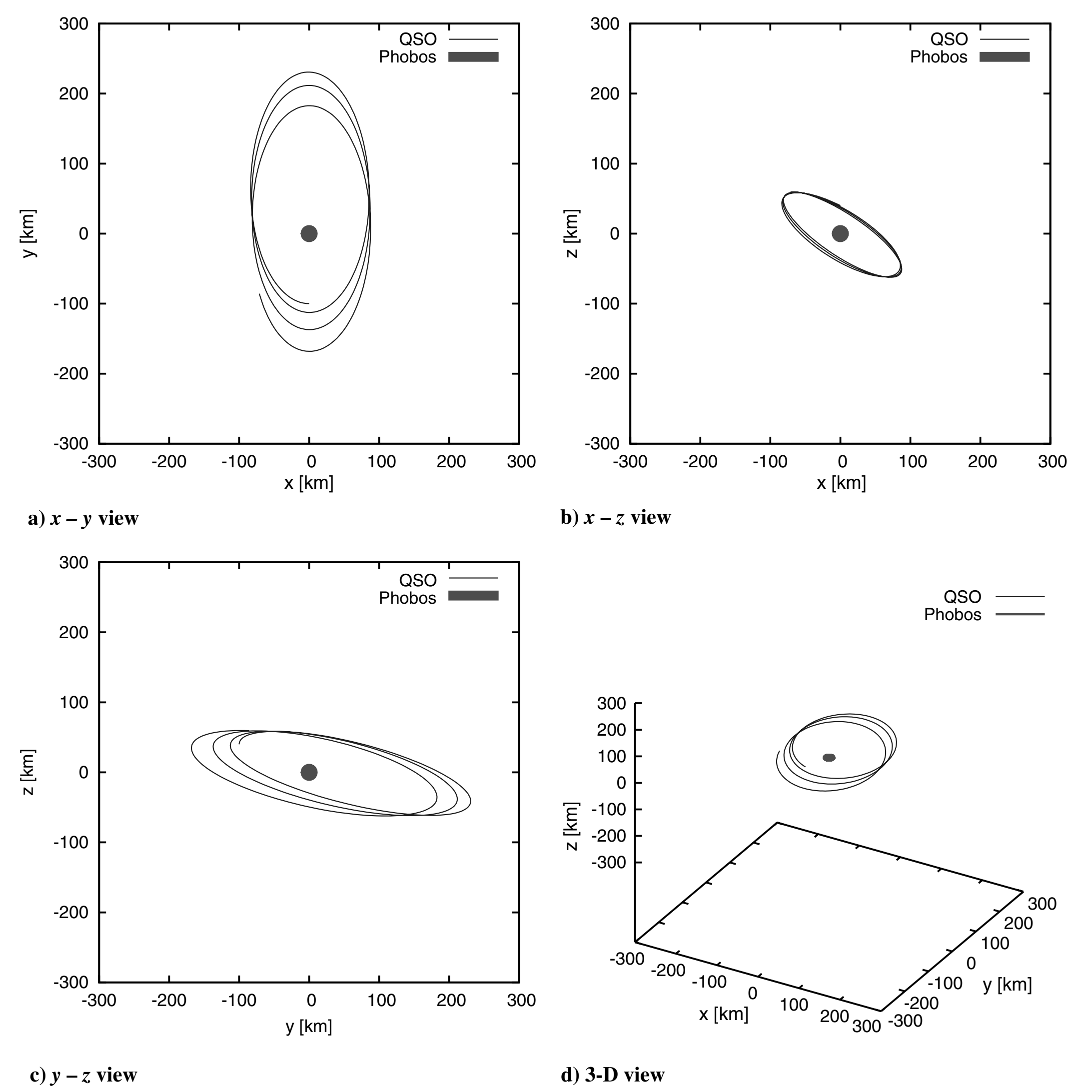


**Fig. 13 The first day of simulation of a 3-D QSO. The drift of the epicycles is initially small and it seems possible that the zone in which the trajectory evolves is limited.**

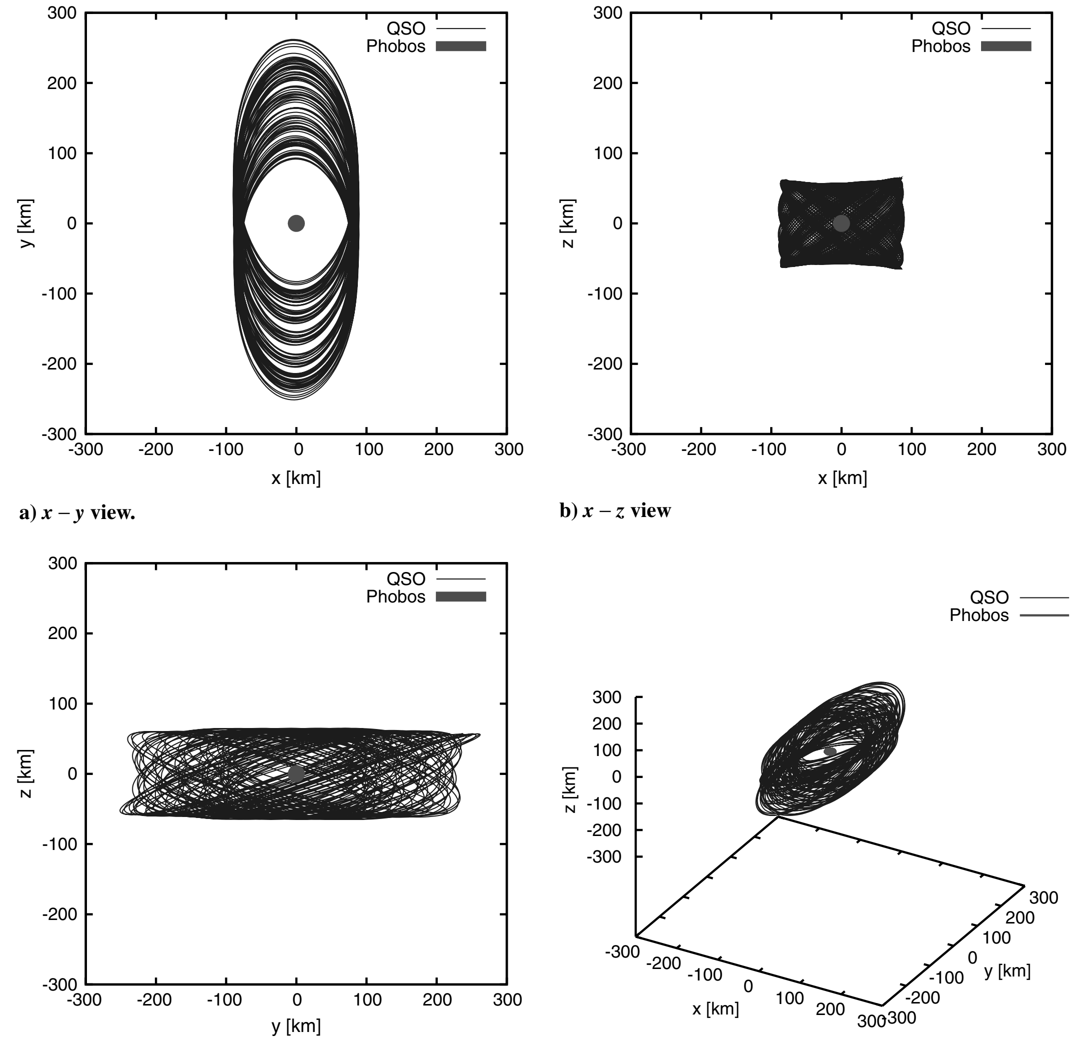


a) $x - y$ view. b) $x - z$ view

c) $y - z$ view d) 3-D view

**Fig. 14 Simulation of a 3-D QSO for 30 days. The zone in which the trajectory evolves was revealed to be extensive because the epicycle plane twists, due to a large variation of the parameter $\psi$.**

sun for long periods of time. For every set of initial conditions, including epoch, this situation must be checked.

### B. Ground Track

The ground track on the Phobos surface of the previously studied 3-D QSO is depicted in Fig. 16a for just one day and in Fig. 16b for 30 days. The latitudes reached are as high as 35° with an elevation angle of the S/C seen from the pole of Phobos of about 25°. This is high enough for reasonable observations of the poles, opening the option of a polar landing. A comparison of the two images in Fig. 16 illustrates that the orientation of the plane of the epicycle slowly changes such that the ground track ultimately covers an entire band between the maximum and minimum latitudes.

A point worth mentioning is that the coverage of the surface takes some time to be completed. Figure 16a suggests that the first epicycles are alike and that only later the trajectory extends to other regions. Figure 13, especially Figs. 13b and 13c, also show that it takes a while for the epicycle to build up an inclination, such that certain regions remain initially uncovered.

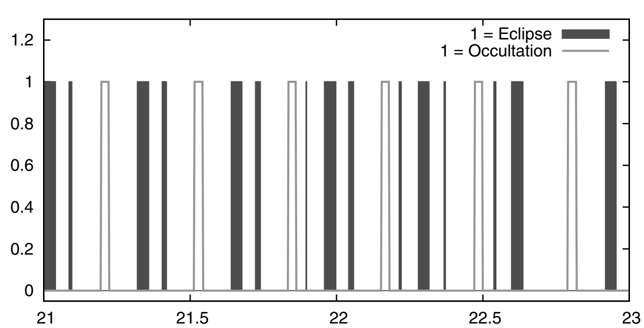


**Fig. 15 Eclipse and occultation events on selected days of the simulation. Two eclipse durations are clearly observed, with the shorter one originated by Phobos instead of Mars.**

### C. Surface Illumination

One important aspect of observation orbits is the illumination status of the surface beneath the S/C. Figures 17a–17c show the elevation of the sun at the ground track of the S/C over several days. Figure 17d shows what happens over the whole 30 days of the simulation.

The results are striking. In general, there are alternating periods of day and night with the approximate orbital period of Phobos. Apart from that, it was found that the elevation of the sun at the ground track can be very small for long periods of time. Even worse, conditions of illumination vary considerably with the sun also reaching very high elevations. As a consequence, the observation conditions undergo large fluctuations. Additionally, the sun remains below the horizon of the instantaneous ground track for approximately 10 days in a row. Overall, the surface beneath the S/C is not at

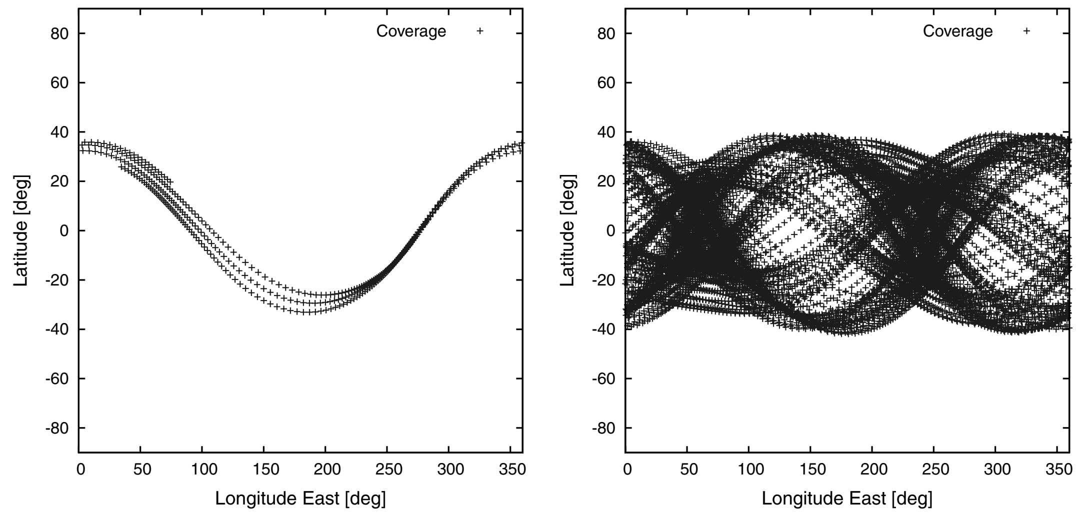


**a) First day of simulation**

**b) 30 days of simulation**

**Fig. 16 Ground track on Phobos of an S/C in a 3-D QSO. The S/C is able to reach considerably high latitudes, enabling the observation of the poles. The surface below the maximum latitude reached is almost completely covered.**

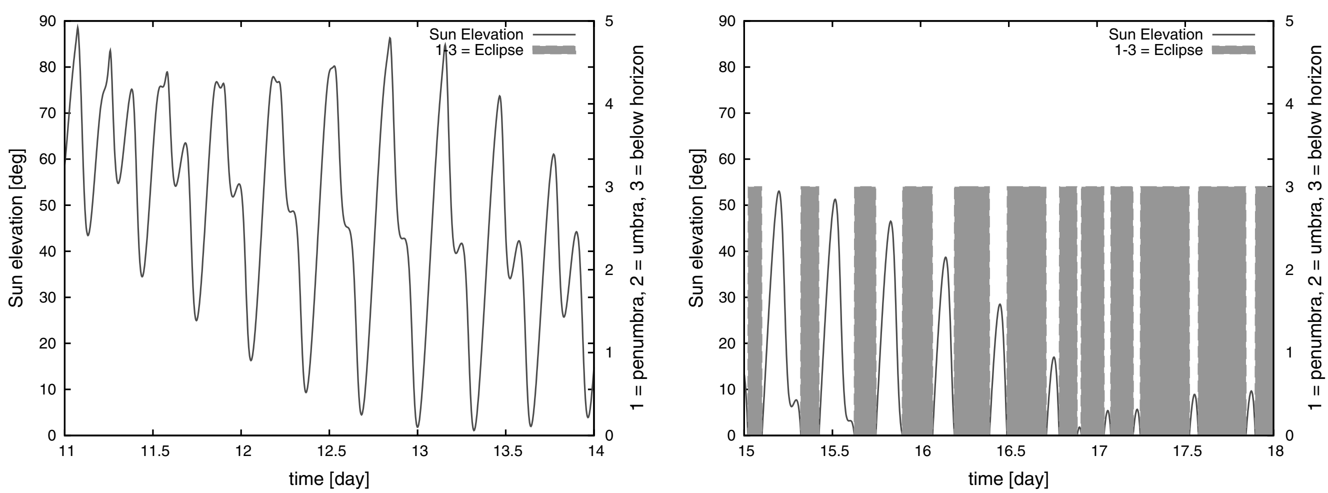


**a) Sometimes the surface is permantly illuminated although the elevation varies extremely**

**b) The periodic illumination varies in duration and maximum angle of elevation**

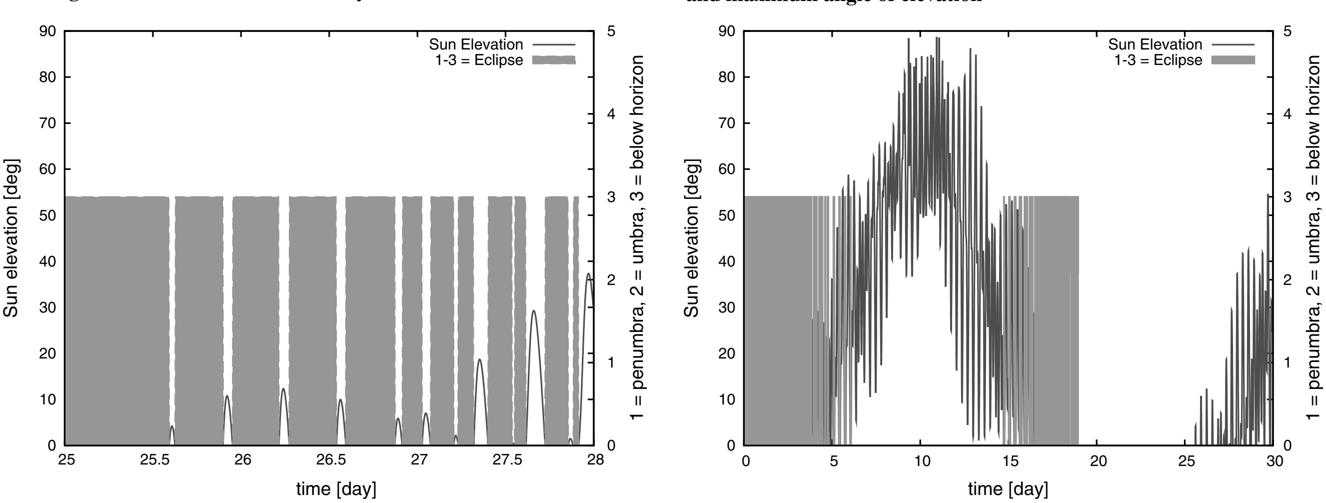


**c) The sun sometimes still appears for short periods of time but remains too low for good observations**

**d) Thirty-day simulation. There are long periods with no illumination of the surface beneath the S/C**

**Fig. 17 Sun elevation angle at the ground track point: a–c) on selected days, and d) for the complete simulation. The elevation exhibits huge variations and there are long periods with the sun below the horizon, obviating observation.**

all illuminated for about half of the time, and during the rest of the time illumination conditions vary a lot, making the window for good observation conditions fairly small.

## VII. Conclusions

The present study aimed at assessing the most important issues regarding QSOs in the context of an SRM to Phobos. A limited but successful phase space scan was performed, as a result of which a number of QSOs were found that are sufficiently stable. The used method suggests a way to enhance the search: a change in the order of the varied parameters may lead to new insights by emphasizing the dependence on each velocity component.

An initial assessment of the precision requirements on the insertion velocity of an S/C into a QSO was performed. It showed that, at least at the examined insertion point, the requirement is of the order of a few meters per second. The velocity component toward Phobos, however, needs to be more accurate, of the order of 1 m/s. More stringent values are found in the literature, the probable explanation being a different insertion point choice (the $x$ axis, contrary to the $y$ axis, which we used in our work).

Other identified features of QSOs around Phobos included the dependency of the QSO period on the distance to Phobos and the dependency of the maximum and minimum altitudes of an S/C in a QSO on its initial distance to Phobos and its initial velocity. However, the obtained results are not sufficiently comprehensive to draw any definite conclusions.

It was found to be more difficult to obtain small QSOs than large ones. A possible cause is the higher-order terms of Phobos's gravitational potential. A heuristic analysis of the relative importance of the forces involved, taking into account the large value of the Phobos $J_2$ term, seems to confirm this claim.

Several 3-D QSOs were simulated and analyzed. The possibility of observing the Phobos poles was verified. The illumination of the ground track and the sun elevation were examined. The results show that long periods of time without adequate illumination of the surface may be encountered, which must be taken into consideration when deciding on an epoch for the mission.

Although computers are becoming increasingly faster, the mixed approach used for Phobos–Grunt of performing numerical simulations as well as theoretical analysis is probably still the best. The latter provide physical insights into the problem, whereas the former are necessary to cover the vast phase space and take into account all the important perturbations.

With these numerical simulations, a broader exploration of the phase space needs to be undertaken to confirm the preliminary results presented here.

The $y$ axis region seems to be the preferable insertion point into a QSO as it appears to be more forgiving to insertion errors. This claim, however, still needs to be confirmed because the transfer geometry is not obvious and possible advantages can strongly depend on details of the mission, such as the position of the sun and the Earth at the time of insertion, the S/C attitude required by the mission, etc. A detailed scheme to insert an S/C into a suitable QSO from further away must also be developed, taking into account this result.

There is a need to further develop the classification scheme of QSOs, similar to the one developed for Phobos–Grunt, which takes into account the 3-D QSO geometry. The fast Lyapunov indicator maps technique [29–31] can be of assistance here. Another issue is the implementation of maneuvers to better study not only the insertion into a QSO but also orbit corrections, changing from one QSO to another, and safe landing procedures.

Additional studies of the 3-D QSOs from a theoretical point of view would be of much value. The top priority should be the prediction of the rate of change of $\psi$ and the value of the critical inclination. An extended knowledge of the 3-D case would allow for a polar landing site or at least a better coverage of high latitude regions.

Regarding in particular the illumination beneath the S/C and eclipse and occultation conditions, it is desirable to simulate QSOs for different times of the year. This is necessary to examine the differences induced by various relative orientations of the orbital plane of Phobos with respect to the sun and the Earth.

Many missions to asteroids and comets of the solar system are currently under consideration and the application of QSOs should be investigated in that framework. Their geometry could provide new possibilities of exploring these small bodies. For example, a QSO could serve as a zero-maintenance orbit that slowly passes through, or avoids, specific regions around the body, such as the outgassing tail of a comet.

## Acknowledgments

The authors would like to thank the anonymous referees for their insightful comments and suggestions. The authors wish to thank Michael Khan for his help and valuable discussions regarding this work. We would also like to thank Valery Lainey for a helpful discussion about ephemerides. The work of Paulo Gil was partially developed during a sabbatical leave at European Space Operations Centre, supported in part by the Fundação para a Ciência e Tecnologia.

## References

[1] Mukhin, L. M., Sagdeev, R., Karavasili, K., and Zakharov, A., "Phobos, Deimos Mission," *Concepts and Approaches for Mars Exploration*, edited by N. G. Barlow, July 2000, pp. 230–232.

[2] Sagdeev, R. Z., and Zakharov, A. V., "Brief History of the PHOBOS Mission," *Nature (London)*, Vol. 341, Oct. 1989, pp. 581–585. doi:10.1038/341581a0

[3] Benest, D., "Libration Effects for Retrograde Satellites in the Restricted Three-Body Problem. I: Circular Plane Hill's Case," *Celestial Mechanics*, Vol. 13, March 1976, pp. 203–215. doi:10.1007/BF01232724

[4] Kogan, A. I., "Distant Satellite Orbits in the Restricted Circular Three-Body Problem," *Cosmic Research (Translation of Kosmicheskie Issledovaniya)*, Vol. 26, June 1989, pp. 705–710.

[5] Lidov, M. L., and Vashkov'yak, M. A., "On Quasi-Satellite Orbits in a Restricted Elliptic Three-Body Problem," *Astronomy Letters*, Vol. 20, Sept. 1994, pp. 676–690.

[6] Kogan, A. I., "Quasi-Satellite Orbits and Their Applications," *Proceedings of the 41st Congress of the International Astronautical Federation*, edited by R. Jehn, International Astronautical Federation Paper 90-307, Oct. 1990.

[7] Marov, M. Y., Avduevsky, V. S., Akim, E. L., Eneev, T. M., Kremnev, R. S., Kulikov, S. D., Pichkhadze, K. M., Popov, G. A., and Rogovsky, G. N., "Phobos–Grunt: Russian Sample Return Mission," *Advances in Space Research*, Vol. 33, 2004, pp. 2276–2280. doi:10.1016/S0273-1177(03)00515-5

[8] Akim, E. L., Zaslavskii, G. S., Morskoi, I. M., Stepan'yants, V. A., and Tuchin, A. G., "Ballistics, Navigation, and Control of Flight of a Spacecraft in the Phobos-Sample-Return Project," *Journal of Computer and Systems Sciences International*, Vol. 41, No. 5, 2002, pp. 818–826; also *Izvestiya Akademii Nauk. Teoriya i Sistemy Upravleniya*, No. 5, pp. 153–161, 2002.

[9] Tuchin, A. G., Akim, E. L., Botkin, A. V., Stepaniants, V. A., Shishov, V. A., and Ruzskiy, E. G., "Orbit Selection, Navigation and Maneuvers Before the Landing on the Phobos Surface for Phobos Sample Return Project," *Proceedings of the 17th International Symposium on Space Flight Dynamics*, Vol. 1, Keldysh Inst. of Applied Mathematics, Moscow, 2003, pp. 291–304.

[10] Akim, E. L., Ruzskiy, E. G., Shishov, V. A., Stepaniants, V. A., and Tuchin, A. G., "Ballistics, Navigation and Motion Control of the S/C on Stages of the Phobos Surface Approaching and Landing," *Proceedings of the 18th International Symposium on Space Flight Dynamics*, Vol. 548, ESA, Paris, 2004, pp. 461–466.

[11] Akim, E. L., Popov, G. A., and Tuchin, A. G., "Mechanics and Motion Control of a Space Vehicle in the Project of Relict Substance Delivery on Earth (The Project "Phobos–Grunt")," *Proceedings of the 16th IFAC Symposium on Automatic Control in Aerospace*, edited by A. Nebylov, Vol. 1, International Inst. for Advanced Aerospace Technologies of State Univ. of Aerospace Information, Saint-Petersburg, Russia, 2004, pp. 209–214.

[12] Szebehely, V., *Theory of Orbits: The Restricted Problem of Three Bodies*, Academic Press, New York/London/Orlando, FL, 1967.

[13] Mikkola, S., Brasser, R., Wiegert, P., and Innanen, K., "Asteroid 2002 VE68, a Quasi-Satellite of Venus," *Monthly Notices of the Royal Astronomical Society*, Vol. 351, July 2004, pp. L63–L65.

doi:10.1111/j.1365-2966.2004.07994.x
[14] Wiegert, P., Innanen, K., and Mikkola, S., "The Stability of Quasi Satellites in the Outer Solar System," *Astronomical Journal*, Vol. 119, April 2000, pp. 1978–1984.
doi:10.1086/301291
[15] Wiesel, W. E., "Stable Orbits About the Martian Moons," *Journal of Guidance, Control, and Dynamics*, Vol. 16, No. 3, 1993, pp. 434–440.
doi:10.2514/3.21028
[16] Hénon, M., "Numerical Exploration of the Restricted Problem. VI. Hill's Case: Non-Periodic Orbits," *Astronomy and Astrophysics*, Vol. 9, Nov. 1970, pp. 24–36.
[17] Benest, D., "Effects of the Mass Ratio on the Existence of Retrograde Satellites in the Circular Plane Restricted Problem," *Astronomy and Astrophysics*, Vol. 32, April 1974, pp. 39–46.
[18] Benest, D., "Effects of the Mass Ratio on the Existence of Retrograde Satellites in the Circular Plane Restricted Problem. II," *Astronomy and Astrophysics*, Vol. 45, Dec. 1975, pp. 353–363.
[19] Benest, D., "Effects of the Mass Ratio on the Existence of Retrograde Satellites in the Circular Plane Restricted Problem. III," *Astronomy and Astrophysics*, Vol. 53, Dec. 1976, pp. 231–236.
[20] Benest, D., "Effects of the Mass Ratio on the Existence of Retrograde Satellites in the Circular Restricted Problem. IV—Three-Dimensional Stability of Plane Periodic Orbits," *Astronomy and Astrophysics*, Vol. 54, Jan. 1977, pp. 563–568.
[21] Dermott, S. F., and Murray, C. D., "The Dynamics of Tadpole and Horseshoe Orbits. I—Theory," *Icarus*, Vol. 48, Oct. 1981, pp. 1–11.
doi:10.1016/0019-1035(81)90147-0
[22] Namouni, F., "Secular Interactions of Coorbiting Objects," *Icarus*, Vol. 137, Feb. 1999, pp. 293–314.
doi:10.1006/icar.1998.6032
[23] Connors, M., Chodas, P., Mikkola, S., Wiegert, P., Veillet, C., and Innanen, K., "Discovery of an Asteroid and Quasi-Satellite in an Earth-Like Horseshoe Orbit," *Meteoritics & Planetary Science*, Vol. 37, Oct. 2002, pp. 1435–1441.
doi:10.1111/j.1945-5100.2002.tb01039.x
[24] De Broeck, P., "Stable Relative Motion as a Solution of the Restricted Three-Body Problem," European Space Operations Centre, ESA Orbit and Attitude Division Working Paper 399, Darmstadt, Germany, 1989.
[25] Lidov, M. L., and Vashkov'yak, M. A., "Perturbation Theory and Analysis of the Evolution of Quasi-Satellite Orbits in the Restricted Three-Body Problem," *Cosmic Research* (translation of *Kosmicheskie issledovaniia*), Vol. 31, April 1993, pp. 75–99.
[26] Russell, R. P., "Global Search for Planar and Three-Dimensional Periodic Orbits Near Europa," *Journal of the Astronautical Sciences*, Vol. 54, No. 2, 2006, pp. 199–226.
[27] Utashima, M., "Design of Phobos-Rendezvous Orbit and its Stability," *Proceedings of the 44th Congress of the* , edited by J. A. S. Elia, International Astronautical Federation Paper 93-A.6.50, Oct. 1993.
[28] Demeyer, J., and Gurfil, P., "Transfer to Distant Retrograde Orbits Using Manifold Theory," *Journal of Guidance, Control, and Dynamics*, Vol. 30, No. 5, 2007, pp. 1261–1267.
doi:10.2514/1.24960
[29] Lara, M., Russell, R. P., and Villac, B., "Fast Estimation of Stable Regions in Real Models," *Meccanica*, Vol. 42, No. 5, 2007, pp. 511–515.
doi:10.1007/s11012-007-9060-z
[30] Lara, M., Russell, R., and Villac, B., "Classification of the Distant Stability Regions at Europa," *Journal of Guidance, Control, and Dynamics*, Vol. 30, No. 2, 2007, pp. 409–418.
doi:10.2514/1.22372
[31] Villac, B. F., "Using FLI Maps for Preliminary Spacecraft Trajectory Design in Multi-Body Environments," *Celestial Mechanics and Dynamical Astronomy*, Vol. 102, Sept. 2008, pp. 29–48.
doi:10.1007/s10569-008-9158-1